Computer-Aided Segmentation and Volumetry of Artificial Ground-Glass Nodules at Chest CT

Ernst Th. Scholten[1,2]
Colin Jacobs[3,4]
Bram van Ginneken[4]
Martin J. Willemink[1]
Jan-Martin Kuhnigk[3]
Peter M. A. van Ooijen[5]
Matthijs Oudkerk[5]
Willem P. Th. M. Mali[1]
Pim A. de Jong[1]

OBJECTIVE. The purpose of this study was to investigate a new software program for semiautomatic measurement of the volume and mass of ground-glass nodules (GGNs) in a chest phantom and to investigate the influence of CT scanner, reconstruction filter, tube voltage, and tube current.

MATERIALS AND METHODS. We used an anthropomorphic chest phantom with eight artificial GGNs with two different CT attenuations and four different volumes. CT scans were obtained with four models of CT scanner at 120 kVp and 25 mAs with a soft and a sharp reconstruction filter. On the 256-MDCT scanner, the tube current–exposure time product and tube voltage settings were varied. GGNs were measured with software that automatically segmented the nodules. Absolute percentage error (APE) was calculated for volume, mass, and density. Wilcoxon signed rank, Mann-Whitney *U*, and Kruskal-Wallis tests were used for analysis.

RESULTS. Volume and mass did not differ significantly from the true values. When measurements were expressed as APE, the error range was 2–36% for volume and 5–46% for mass, which was significantly different from no error. We did not find significant differences in APE between CT scanners with filters for lower tube current for volume or lower tube voltage for mass.

CONCLUSION. Computer-aided segmentation and mass and volume measurements of GGNs with the prototype software had promising results in this study.

Keywords: CT, ground-glass opacity nodule, volume measurement

DOI:10.2214/AJR.12.9640

Received July 20, 2012; accepted after revision September 11, 2012.

J. M. Kuhnigk received funding for research from the Federal Ministry of Education and Research, Germany. C. Jacobs received a research grant from MeVis Medical Solutions AG, Germany.

[1]Department of Radiology, University Medical Centre Utrecht, Heidelberglaan 100, 3584 CX Utrecht, The Netherlands. Address correspondence to E. Th. Scholten (ethscholten@quicknet.nl).

[2]Department of Radiology, Kennemer Gasthuis, Haarlem, The Netherlands.

[3]Fraunhofer MeVis, Bremen, Germany.

[4]Department of Radiology Image Analysis Group, University Medical Centre, St Radboud, Nijmegen, The Netherlands.

[5]Department of Radiology, University of Groningen, University Medical Centre, Groningen, The Netherlands.

AJR 2013; 201:295–300

0361–803X/13/2012–295

Nonsolid or ground-glass nodules (GGNs) are a major challenge, both clinically [1] and in lung cancer screening trials, because these nodules are far less common than solid nodules, are slow-growing, are often multiple, and have a high malignancy rate. For example, in the Early Lung Cancer Action Project study [2], 19% of cases of positive screening results involved pure or partly solid GGNs. In the first round of the Dutch-Belgian lung cancer screening trial [3], only 2.0% of the total of 8673 nodules found in 7557 participants were pure nonsolid nodules or partly solid GGNs. Growth rates with a mean volume doubling time of 813 days and malignancy rates up to 63% have been reported for pure GGNs [2, 4].

A GGN is defined as an area of increased lung attenuation with preservation of the bronchial and vascular margins [5]. Given the slow growth rate, the diagnosis of growing GGNs is challenging. According to results of a study by de Hoop et al. [6], measurements of mass can lead to earlier detection of growth of GGNs than can volume and diameter measurements. Mass measurements were obtained through manual segmentation on axial CT images followed by calculation of volume with the computer. GGN mass was then calculated with the attenuation values expressed in terms of physical density. These manual measurements require approximately 5–10 minutes of segmentation time. Development of a more automated method for segmentation of these nodules would be a major scientific advance.

In this study, using a chest phantom with eight nodules of different size and density, we investigated a software program that automatically segments GGNs and allows adjustment of roundness and density and then calculates volume and mass. We also investigated the influence of CT machine, reconstruction algorithm, tube voltage, and tube current on the measurements.

Materials and Methods

Phantom

An anthropomorphic thorax phantom (Lungman, Kyoto Kagaku) with artificial heart, lung vessels,

thoracic wall, diaphragm, and liver was used. The phantom consists of an accurate life-size anatomic model of a male torso with soft-tissue substitute materials made of polyurethane resin composites and synthetic bones made of epoxy resin with x-ray absorption rates close to those of human tissue. The space between the lung vessels in the thoracic cavity consisted of air. We inserted eight artificial spherical homogeneous lung nodules with a smooth surface that were supplied by the manufacturer in four diameters (5, 8, 10, and 12 mm, corresponding to volumes of 65, 268, 523, and 904 mm^3) and two CT attenuations (–800 and –630 HU). Table 1 and Figure 1 show all nodule characteristics and locations in the phantom. The artificial nonsolid nodules were made of polyurethane foam resin.

TABLE 1: Characteristics of the Eight Ground-Glass Nodules in the Phantom

Nodule No.	Attenuation (HU)	Diameter (mm)	Volume (mm^3)	Weight (mg)	Perivascular
1	–800	5	65.4	13.1	Partially
2	–800	8	268.1	53.6	No
3	–800	10	523.6	104.7	Yes
4	–800	12	904.8	181.0	Completely
5	–630	5	65.4	24.2	Yes
6	–630	8	268.1	99.2	Partially
7	–630	10	523.6	193.7	No
8	–630	12	904.8	334.8	Partially

CT Protocol

CT images were obtained with four systems: two 16-MDCT scanners (Mx8000 IDT and Brilliance 16P, Philips Healthcare), one 64-MDCT scanner (Brilliance 64, Philips Healthcare), and one 256-MDCT scanner (Brilliance iCT, Philips Healthcare). For all CT acquisitions, the same slice thickness of 1 mm was used. CT with all four machines was performed at a tube voltage of 120 kVp and tube current–time product of 25 mAs. These settings are typical for a low-dose protocol [3].The CT images were reconstructed with soft (b) and sharper (c) filters. Thus eight sets of images obtained with this standard technique were available for evaluation. To determine the influence of tube voltage and tube current on the accuracy of the mass measurements, we varied the tube current–time product setting at 25 mAs and the voltage at

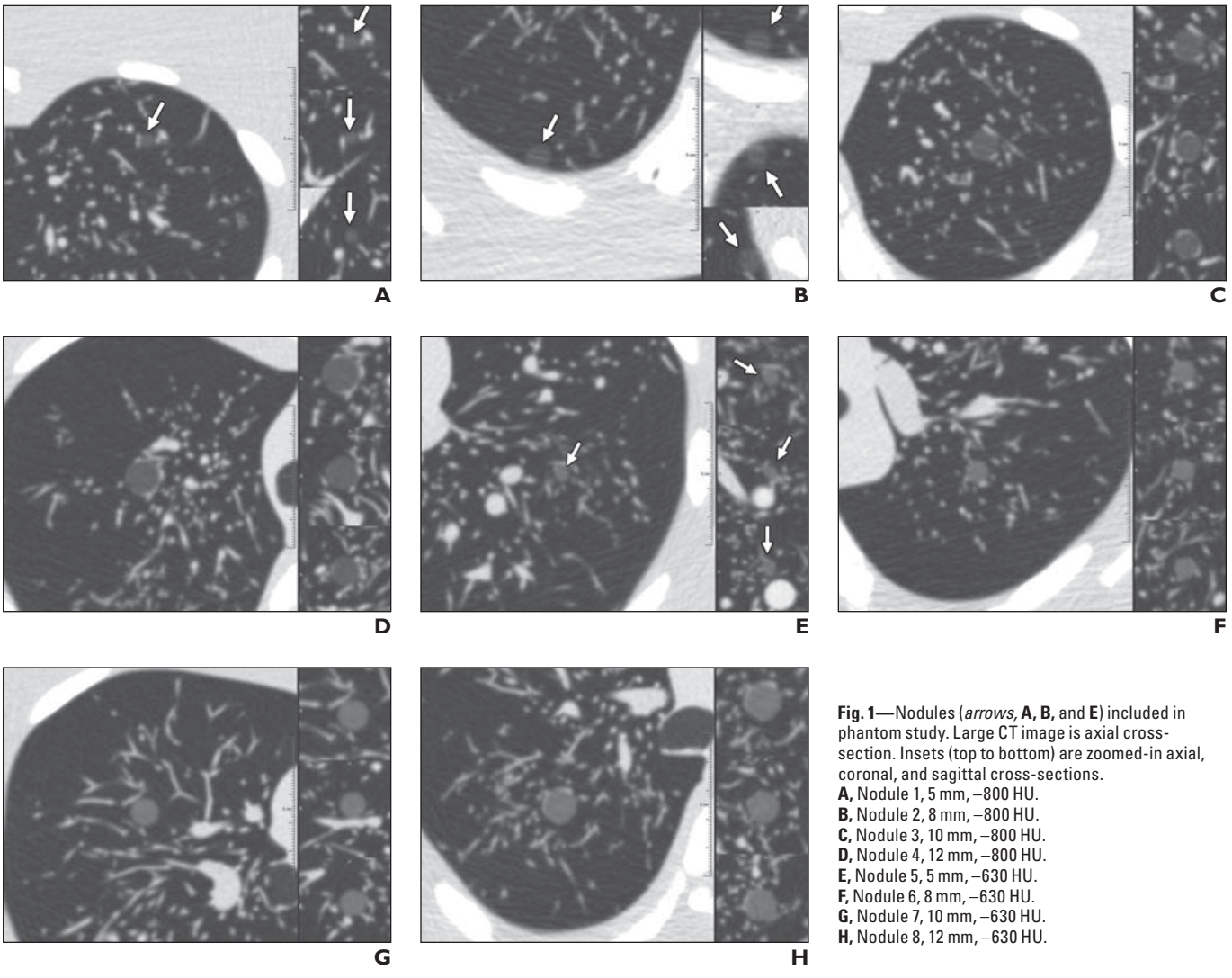

Fig. 1—Nodules (*arrows,* **A, B,** and **E**) included in phantom study. Large CT image is axial cross-section. Insets (top to bottom) are zoomed-in axial, coronal, and sagittal cross-sections.
A, Nodule 1, 5 mm, –800 HU.
B, Nodule 2, 8 mm, –800 HU.
C, Nodule 3, 10 mm, –800 HU.
D, Nodule 4, 12 mm, –800 HU.
E, Nodule 5, 5 mm, –630 HU.
F, Nodule 6, 8 mm, –630 HU.
G, Nodule 7, 10 mm, –630 HU.
H, Nodule 8, 12 mm, –630 HU.

TABLE 2: CT Acquisition Protocols

Setting	Brilliance 16P		Brilliance iCT 256						Brilliance 64		Mx8000 IDT	
Tube voltage (kVp)	120	120	80	100	120	120	120	120	120	120	120	120
Tube current–time product (mAs)	25	25	25	25	100	50	25	25	25	25	25	25
Filter	b	c	c	c	c	c	c	b	b	c	b	c

Note—All scanners are products of Philips Healthcare.

120 kVp on the Brilliance iCT scanner for a total of seven combinations (Table 2). All scans were obtained sequentially on a single day without change in the position of the nodules in the phantom.

Ground-Glass Nodule Quantification Protocol

The lung nodules were measured by one reader, a radiologist with 30 years of experience, using a standard PC running prototype software (Fraunhofer MeVis, Diagnostic Image Analysis Group). The algorithm was based on previously published techniques for segmentation of solid pulmonary nodules [7]. When the user placed a cursor on the nodule of interest and clicked with the mouse, the software automatically delineated the nodule and quantified its diameter, volume, average density, and mass. Two parameters, density threshold value and roundness of the segmentation, can be adjusted by the user. Density threshold values for the nodule segmentation were set to –850 HU as the lower limit and –150 HU as the upper limit. Roundness was a shape parameter of the segmentation with a value range between 0 and 100%. When the value is decreased, a more irregular boundary of segmentation is allowed. When the roundness value is increased, the boundary of the segmentation becomes smoother. Adjustments take the time of a mouse click, and updated results are instantly presented to the user.

A first measurement was performed with the default values of the program without further adjustment by the observer. Measurements were subjectively rated on a 5-point scale as follows: complete failure (no measurement possible), poor (gross underestimation or overestimation of the nodule), fair (evident imperfections), good (small visible imperfections), and perfect. A second measurement was made if the result of the first measurement was considered less than perfect. In the second measurement the observer was allowed to adjust roundness and density thresholds. Enlarged multiplanar reconstructions in three directions presented simultaneously with the axial image were used to judge the quality of the segmentation and to judge the effect of the adjustments (Fig. 2).

Data and Statistical Analysis

Absolute percentage error (APE) was used to evaluate measurement accuracy [8]. This APE was calculated as follows:

$$APE = 100\% \times \frac{value_{measured} - value_{true}}{value_{true}}.$$

For the eight measurements with our standard technique, mean APE values were calculated for the measured average density, volume, and mass of the nodule. Deviations of the measurements from the known nodule density, volume, and mass and of the APE from zero error were analyzed with descriptive statistics as median ± interquartile range, graphically, and by use of the Wilcoxon signed rank test. Differences between protocols and CT machines were analyzed by Mann-Whitney *U* test and Kruskal-Wallis test. Only one nodule had a measurement failure even after adjustment (nodule 2, Brilliance 64 CT scanner, 125 kVp, 25 mAs, c filter), so this attempted measurement was not included in further analysis. A value of $p < 0.05$ was considered significant.

Results

Ground-Glass Nodule Measurements

Without any adjustment 37 of 64 (57.8%) measurements in our series with 25 mAs and 120 kVp were perfect (eight measurements) or good (29 measurements). After adjustment of roundness and density, 58 of 64 (90.6%) measurements were perfect or good, and six (9.4%) were considered fair, poor, or failure.

Ground-Glass Nodule Attenuation, Volume, and Mass Measurements at 120 kVp and 25 mAs With Soft and Sharper Filters

Mean density APE ranged from 2% for the 5-mm –800-HU nodule to 11% for the 8-mm –800-HU nodule. Mean volume APE ranged from 2% for the 10-mm –630-HU nodule to 36% for the 5-mm –800-HU nodule. Mean mass APE ranged from 5% (12-mm nodule) to 17% (5-mm nodule) for the nodules of –630 HU and from 15% (12-mm nodule) to 46% (8-mm nodule) for the –800-HU nodules. The measurements were not significant-

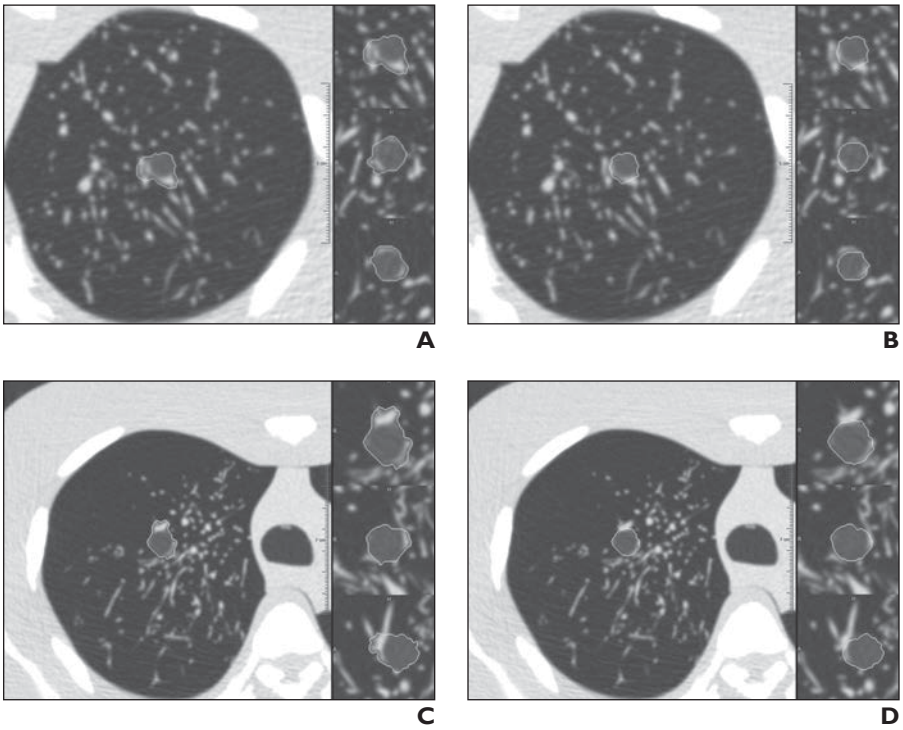

Fig. 2—Exclusion of perivascular vessels by adjustment of roundness.
A–D, CT images show inclusion of several vessel fragments in segmentation. After adjustment of roundness (**B** and **D**), vessel fragments are almost completely excluded.

TABLE 3: Nodule Measurements on CT Scans of the Phantom

Nodule No.	True Value			Measured Value					
	Attenuation (HU)	Volume (mm^3)	Mass (mg)	Attenuation (HU)		Volume (mm^3)		Mass (mg)	
				Median	Interquartile Range	Median	Interquartile Range	Median	Interquartile Range
1	–800	65.4	13.1	–804.3	–808.2 to –785.7	43.8	35.0–67.8	8.7	6.7–14.6
2	–800	268.1	53.6	–696.2	–742.2 to –678.7	278.4	217.7–316.1	68.5	66.2–91.1
3	–800	523.6	104.7	–756.6	–777.9 to –751.4	462.3	420.1–570.2	114.6	93.4–140.4
4	–800	904.8	181.0	–781.3	–789.7 to –773.7	873.2	752.7–951.1	190.9	158.8–213.8
5	–630	65.4	24.2	–690.4	–694.4 to –686.2	65.7	61.4–68.1	20.1	19.0–21.4
6	–630	268.1	99.2	–679.6	–688.1 to –665.6	273.8	267.5–320.2	87.5	82.9–107.2
7	–630	523.6	193.7	–685.0	–688.0 to –681.2	532.1	520.9–538.9	168.6	163.0–170.8
8	–630	904.8	334.8	–653.2	–653.2 to –650.1	967.8	910.6–1013.2	336.9	309.2–353.3

Note—Measured nodule values are the average of eight measurements with the standard technique at 120 kVp and 25 mAs.

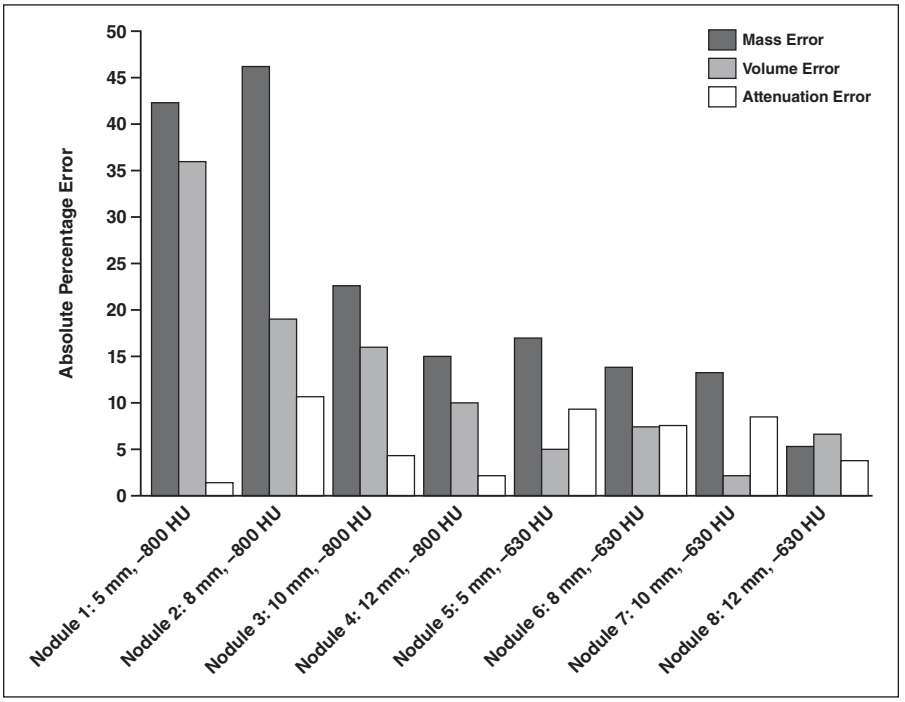

Fig. 3—Graph shows absolute percentage error in mass, volume, and attenuation measurement at 120 kV and 25 mAs.

ly different from the true values. Data are further presented in Table 3 and Figure 3.

Influence of Filters, Voltage, Current, and CT Scanner on Ground-Glass Nodule Measurements

Differences in APE between filters for nodule density, volume, and mass at 120 kVp and 25 mAs were not significant ($p = 0.4$, $p = 0.8$, $p = 0.6$) (Fig. 4). In addition, the tube current–time setting did not significantly influence nodule density, volume, or mass ($p = 0.9$, $p = 0.96$, $p = 0.97$). Decreasing the tube voltage to 80 kVp increased the APE for mass from 28% to 46%. This result must be attributed to the APE for the volume measurement, because the APE for attenuation remained the same (7% for 120 and 80 kVp). The APE for volume increased from 12% to 36%. The errors that can occur at 80 kVp are shown in Figure 5. Obvious noise on the image resulted in underestimation of the volume whereas the attenuation measurement remained accurate. These differences in volume and mass measurements did not reach significance ($p = 0.8$, $p = 0.4$), although the 46% APE was the largest error we observed in any of the CT series. Regarding the four CT acquisitions, we did not find significant differences in APE for attenuation ($p = 0.8$), volume ($p = 0.6$), or mass ($p = 0.8$).

Discussion

Because volumetry is preferable to diameter measurements for quantifying the growth rate of GGNs as an indicator of malignancy [6], we evaluated a prototype software program that semiautomatically measures density, mass, and volume. To the best of our knowledge, our study is the first to focus not only on computer-aided segmentation and volume measurement of GGNs but also on measurement of mass. Our study results are promising in showing the volume and mass measurements of nodules of different sizes and different densities. After easy manual adjustments, overall APE of volume and mass measurements of 5% and 13% was achieved with measurements that are made rapidly, within 1 second of computation time.

There have been limited reports on volume measurements of GGNs [9–11]. Oda et al. [10] reported errors between –4.1% and 7.1% in a study with a different phantom from ours with nodules measuring 5 mm or more. Those authors, however, performed only routine-dose CT, which is not available in the context of screening studies or follow-up studies for clinically detected nodules. We focused on a typical low-dose lung cancer screening protocol using 125 kVp and 25 mAs because that is the context in which most GGNs are found and evaluated in follow-up studies.

Linning and Daqing [11] also varied the tube current–time product setting in a phantom study with tube current ranging from 30 to 210 mA, resulting in a tube current–time product of 15–105 mAs. Their nodules were all fairly large, between 589 and 897 mm^3.

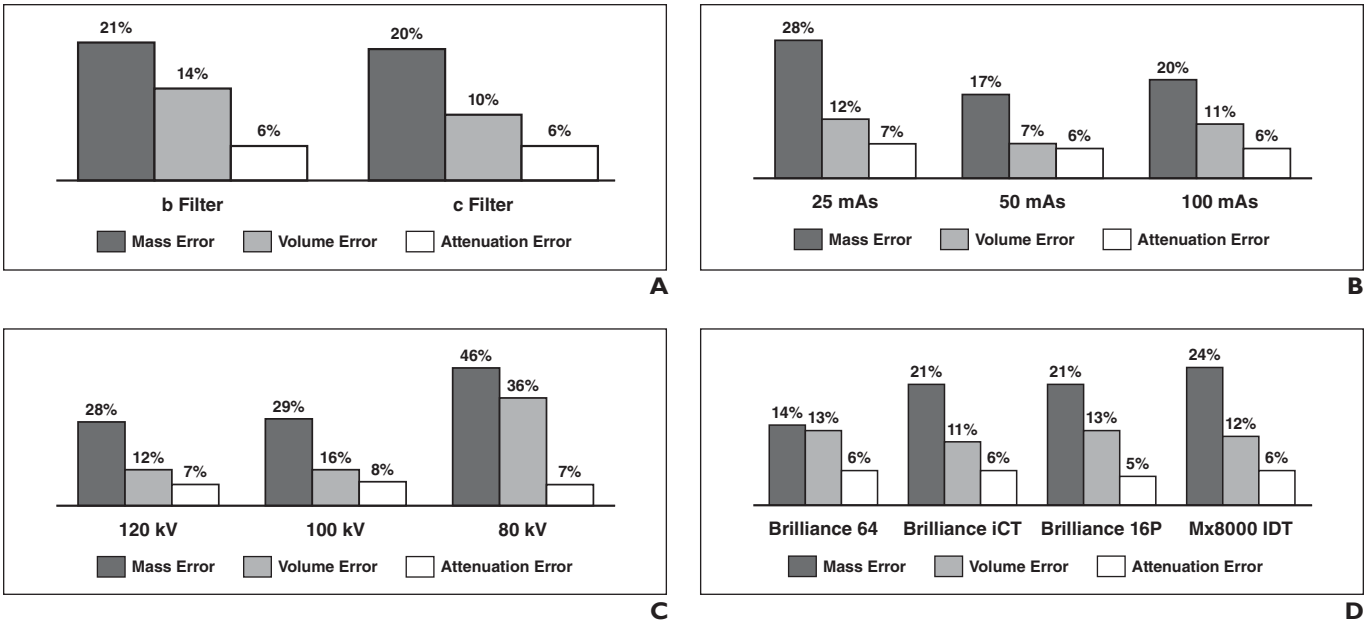

Fig. 4—Graphs show absolute percentage error (APE) in mass, volume, and attenuation measurements under varying conditions.
A, Different reconstruction algorithms at 120 kVp and 25 mAs.
B, Different tube current–time products at 120 kVp.
C, Different tube voltages at 25 mAs.
D, Different scanners (all Philips Healthcare) at 120 kVp and 25 mAs.

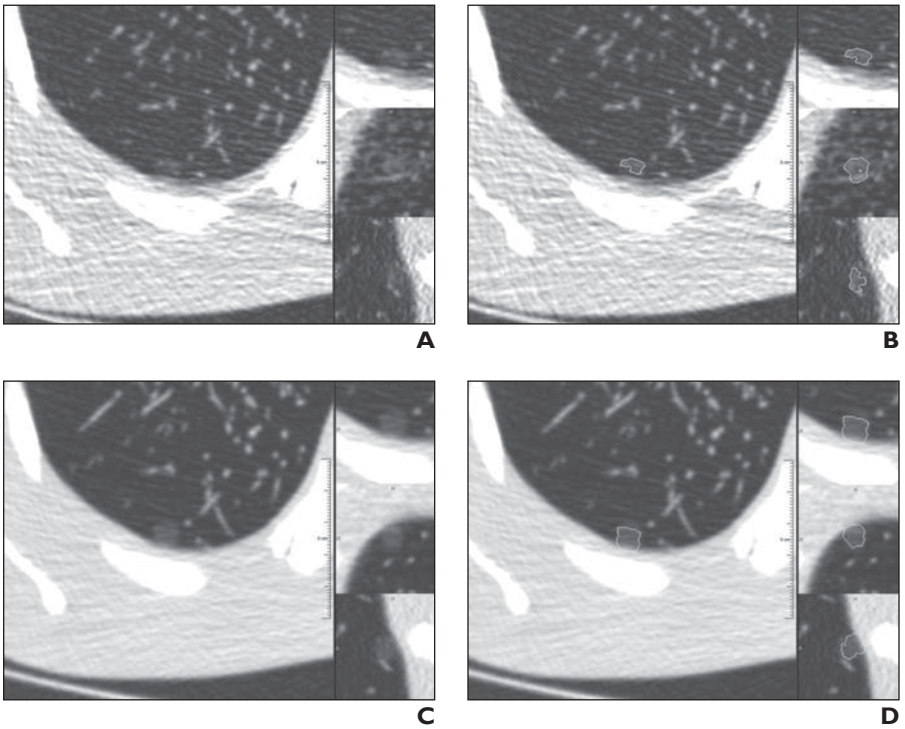

Fig. 5—Nodule 2 (8 mm, –800 HU).
A–D, CT images obtained at 80 kVp (**A** and **B**) and 120 kVp (**C** and **D**) before (**A** and **C**) and after (**B** and **D**) segmentation. Note gross underestimation of volume due to noise on 80-kVp images (**B**). Attenuation measurement remained accurate.

Those investigators reported an APE for volume measurements of 0.14–22.67% with a mean relative percentage error ranging from –7% at 60 mA to 2.32% at 120 mA. Taking into account the substantial differences between the nodules in their study and those in our study, it is difficult to compare our studies. It is important to realize the larger errors in small GGNs at low-dose CT in the evaluation of nodule growth, because growth is defined as an increase in the nodule measurement exceeding the measurement error. This emphasizes the difficulty of using low-dose imaging to diagnose growth of small GGNs.

We did not find significant differences between various generations of CT scanners from a single vendor or between filters. Unlike other authors [12, 13], however, in solid nodules we did find a negative influence of lowering the tube voltage to 80 kVp. This result was not statistically significant, which is probably explained by our small sample size. However, errors increased to 46%, and our impression, as shown in Figure 5, is that dose must be considered more carefully for GGNs than for solid nodules, in which the contrast is much higher and thus less influenced by noise.

Small visible imperfections of the segmentation process were noted in the exclusion of vessels in the nodules in this phantom that had adjacent vessels. Inclusion of part of the vessel artificially raises the apparent mass of a nodule. In clinical practice, this situation would be even more complex because not only vessels adjacent to but also vessels running through a GGN have to be dealt with,

and GGNs can have solid components. Further research into this problem is warranted.

The limitations of the study were mainly those inherent to use of a phantom, which removed any disturbance due to voluntary or involuntary movement of a subject. Nodules in the phantom were truly round, and this may have made it easier to adjust the measurement to an optimal result. Another limitation was that nodules did not contain vessels running through them that could influence the accuracy of the measurements. A third limitation was that even though the nodules in our phantom were surrounded by air and not by lung tissue, the lowest-attenuation nodules differed by only 200 HU from their surroundings, This might explain why measurements in these nodules were less accurate than in the –630-HU nodules.

Conclusion

Computer-aided segmentation and mass measurement of GGNs with the prototype software showed promise in this phantom study. Care must be taken in choosing the technical parameters for CT for GGN quantification because excessive noise on the image can cause inaccurate results.

References

1. Godoy MC, Naidich DP. Subsolid pulmonary nodules and the spectrum of peripheral adenocarcinomas of the lung: recommended interim guidelines for assessment and management. *Radiology* 2009; 253:606–622
2. Henschke CI, Yankelevitz DF, Mirtcheva R, et al. CT screening for lung cancer: frequency and significance of part-solid and nonsolid nodules. *AJR* 2002; 178:1053–1057
3. van Klaveren RJ, Oudkerk M, Prokop M, et al. Management of lung nodules detected by volume CT scanning. *N Engl J Med* 2009; 361:2221–2229
4. Hasegawa M, Sone S, Takashima S, et al. Growth rate of small lung cancers detected on mass CT screening. *Br J Radiol* 2000; 73:1252–1259
5. Hansell DM, Bankier AA, MacMahon H, McLoud TC, Müller NL, Remy J. Fleischner Society: glossary of terms for thoracic imaging. *Radiology* 2008; 246:697–722
6. de Hoop B, Gietema H, van de Vorst S, Murphy K, van Klaveren RJ, Prokop M. Pulmonary ground-glass nodules: increase in mass as an early indicator of growth. *Radiology* 2010; 255:199–206
7. Kuhnigk JM, Dicken V, Bornemann L, et al. Morphological segmentation and partial volume analysis for volumetry of solid pulmonary lesions in thoracic CT scans. *IEEE Trans Med Imaging* 2006; 25:417–434
8. Goo JM, Tongdee T, Tongdee R, et al. Volumetric measurement of synthetic lung nodules with multi-detector row CT: effect of various image reconstruction parameters and segmentation thresholds on measurement accuracy. *Radiology* 2005; 235:850–856
9. Park CM, Goo JM, Lee HJ, et al. Persistent pure ground-glass nodules in the lung: interscan variability of semiautomated volume and attenuation measurements. *AJR* 2010; 195:[web]W408–W414
10. Oda S, Awai K, Murao K, et al. Computer-aided volumetry of pulmonary nodules exhibiting ground-glass opacity at MDCT. *AJR* 2010; 194: 398–406
11. Linning E, Daqing M. Volumetric measurement pulmonary ground-glass opacity nodules with multi-detector CT: effect of various tube current on measurement accuracy—a chest CT phantom study. *Acad Radiol* 2009; 16:934–939
12. Das M, Ley-Zaporozhan J, Gietema HA, et al. Accuracy of automated volumetry of pulmonary nodules across different multislice CT scanners. *Eur Radiol* 2007; 17:1979–1984
13. Way TW, Chan HP, Goodsitt MM, et al. Effect of CT scanning parameters on volumetric measurements of pulmonary nodules by 3D active contour segmentation: a phantom study. *Phys Med Biol* 2008; 53:1295–1312